

J/ψ Radiative Decays

Xiaoyan SHEN
for the BES Collaboration

*Institute of High Energy Physics
Chinese Academy of Sciences
Beijing, P. R. China*

ABSTRACT

The previous results of J/ψ radiative decays from MARKIII, DM2, Crystal Ball and BESII are briefly reviewed in this talk. The main part of this talk focuses on presenting the recent results from BESII 5.8×10^7 J/ψ data, including the Partial Wave Analysis (PWA) results, the measurement of η_c mass, as well as search for some interesting states.

1 Introduction

One of the distinctive features of QCD as a non-Abelian gauge theory is the interaction of quarks and gluons, which predicts the existence of other types of hadrons with explicit gluonic degrees of freedom – glueballs and hybrids. The indirect evidence for gluon-gluon interactions has been obtained at high energies. However, glueballs, the bound states of gluons, and hybrids predicted by QCD, have not been confirmed yet. Therefore, the observation of glueballs and hybrids is, to some extent, a direct test of QCD, and the study of the glueball and hybrid spectroscopy,

together with the meson and baryon spectroscopy will be a good laboratory for the study of the strong interactions in the strongly coupled non-perturbative regime.

Many QCD-based models and calculations, for example, bag models [1], flux-tube models [2], QCD sum rules [3] and lattice QCD [4] are developed to make predictions to the properties of glueballs and hybrids. Of them, lattice QCD is considered as the most relevant since it originated from the first principle of QCD.

According to the calculations of different lattice QCD groups[4], the lightest glueball is found to be a 0^{++} state with the mass in the region of 1.5-1.7 GeV, while the next lightest glueball is a 2^{++} with the mass around 2.3GeV.

J/ψ decay is a good lab. for the study of hadron spectroscopy, as well as glueball and hybrid search. Fig.1 shows the Feymann diagrams of some J/ψ decays. A naive estimation of the production rate of various particles based simply on counting powers of the electromagnetic and strong coupling constants yields,

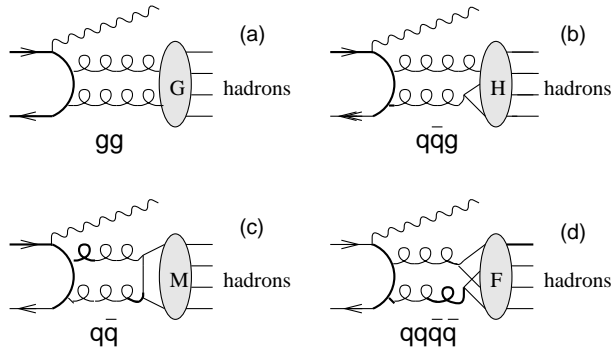


Figure 1: J/ψ decays

$$\Gamma(J/\psi \rightarrow \gamma G) \sim O(\alpha\alpha_s^2), \quad \Gamma(J/\psi \rightarrow \gamma H) \sim O(\alpha\alpha_s^3)$$

$$\Gamma(J/\psi \rightarrow \gamma M) \sim O(\alpha\alpha_s^4), \quad \Gamma(J/\psi \rightarrow \gamma F) \sim O(\alpha\alpha_s^4)$$

where, G, H, M and F represent glueball, hybrid state, meson and four-quark state, respectively. Apparently, glueballs have enhanced production rates in J/ψ radiative decays.

2 Previous results on J/ψ radiative decays

Many experiments at the e^+e^- storage ring facilities, such as Crystal Ball, MARKIII, DM2 and BES have been dedicating to the study of the hadron spectroscopy and the search for non- $q\bar{q}$ states through J/ψ radiative decays.

DASP, MARKII, MARKIII, DM2, Crystal Ball and BES studied the radiative production of $q\bar{q}$ mesons, such as tensors, scalars, pseudoscalars and axialvectors, and measured the resonance parameters, decay branching ratios and polarization parameters. In search for glueballs and new resonances, these experiments provided much information on $f_0(1500)$, $f_0(1710)$, $\iota/\eta(1440)$ and $\xi(2230)$.

3 Preliminary results from BESII J/ψ data

BES, shown in Fig. 2, is a large general purpose solenoidal detector at the Beijing Electron Positron Collider (BEPC). The beam energy range is from 1.0 to 2.8 GeV and the luminosity at J/ψ peak is around $5 \times 10^{30} \text{cm}^{-2} \text{s}^{-1}$. The details of BES I are described in ref. [5]. The upgrades of BES I to BES II [6] include the replacement of

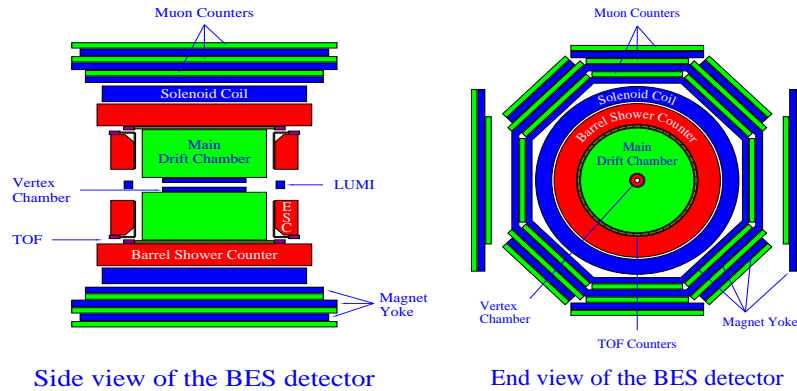


Figure 2: *BES detector*

the central drift chamber with a vertex chamber composed of 12 tracking layers, the installation of a new barrel time-of-flight counter (BTOF) with a time resolution of 180ps and the installation of a new main drift chamber (MDC), which has 10 tracking layers and provides a dE/dx resolution of $\sigma_{dE/dx} = 8.4\%$ for particle identification and $\sigma_p/p = 1.7\% \sqrt{1+p^2}$ (p in GeV) momentum resolution for charged tracks. The barrel shower counter (BSC), which covers 80% of 4π solid angle, has an energy resolution of $\sigma_E/E = 22\%/\sqrt{E}$ (E in GeV) and a spatial resolution of 7.9 mrad in ϕ and 2.3 cm in z , is located outside the TOF. Outermost is a μ identification system, which consists of three double layers of proportional tubes interspersed in the iron flux return of the magnet.

With the upgraded BES II detector, till the summer of 2001, about $5.8 \times 10^7 J/\psi$ events have been accumulated. This is the largest J/ψ data sample in the world. Fig. 3 shows the inclusive K_s^0 and ϕ signals, which indicates a good data quality and a large data sample.

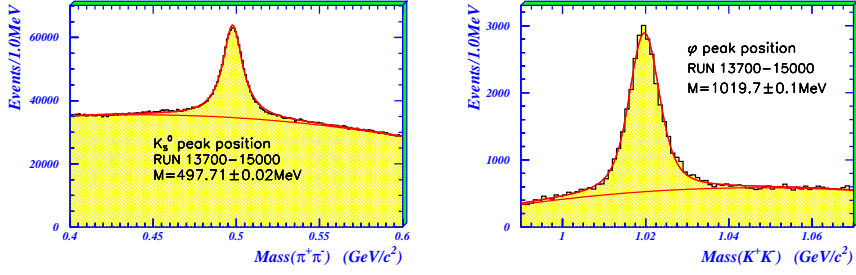


Figure 3: Inclusive K_s^0 and ϕ signals

3.1 Partial Wave Analysis of $J/\psi \rightarrow \gamma K \bar{K}$ (preliminary)

The spin-parity of the structure around 1.7 GeV has a long history of uncertainty. Partial wave analyses (PWA) are applied to $J/\psi \rightarrow \gamma K^+ K^-$ and $\gamma K_s^0 K_s^0$ channels, based on BESII $5.8 \times 10^7 J/\psi$ events. Fig. 4 shows the invariant mass spectra of $K^+ K^-$ and $K_s^0 K_s^0$, where $f_2'(1525)$ and the structure around 1.7 GeV are clearly seen in both cases. The amplitudes are fitted to the relativistic covariant tensor

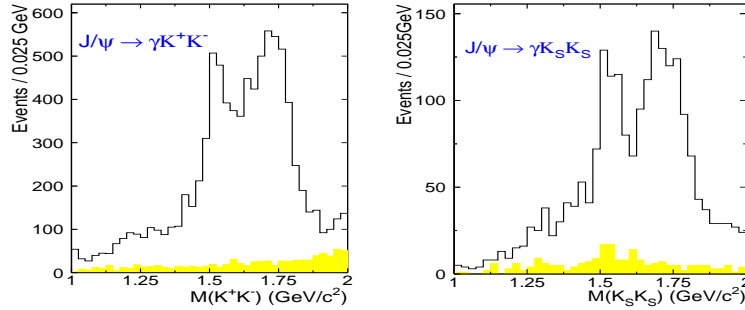


Figure 4: $K^+ K^-$ and $K_s^0 K_s^0$ invariant mass spectra in $J/\psi \rightarrow \gamma K^+ K^-$ and $J/\psi \rightarrow \gamma K_s^0 K_s^0$

expressions, and the maximum likelihood method is applied in the fit. Global and slice fits are performed to KK mass region of 1-2 GeV. For slice fit, 40MeV bin width is adopted. Fig. 5 shows 0^{++} and 2^{++} intensity distributions as a function of the invariant mass of $K^+ K^-$ and $K_s^0 K_s^0$, where, dots with error bars are the efficiency corrected data points, solid curves stand for the coherent superposition of the individual Breit-Wigner resonance fits and dashed histograms represent the global fit results. Both $K^+ K^-$ and $K_s^0 K_s^0$ D wave intensity shows a clear $f_2'(1525)$ with the mass and width being $M = 1518 \pm 6$ MeV and $\Gamma = 84_{-24}^{+28}$ MeV. There is an evidence for $f_2(1270)$ and a weak 2^{++} intensity in the mass region around 1.7 GeV. While 0^{++} is found to be dominant in 1.7 GeV region, which is well determined by

a Breit-Wigner resonance. The mass and width of the 0^{++} component are:

$$M = 1703_{-10}^{+8} \text{ MeV}, \quad \Gamma = 163_{-22}^{+27} \text{ MeV}$$

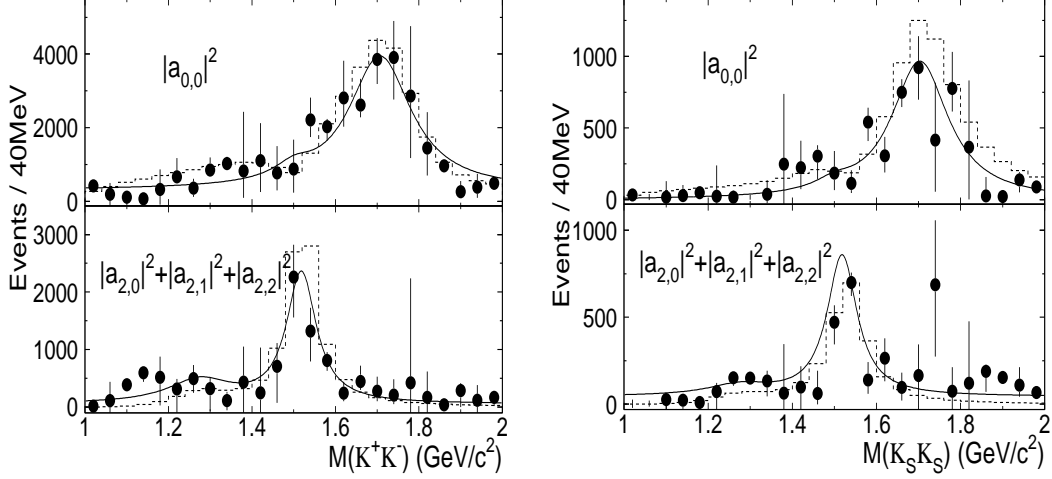


Figure 5: PWA fit results of K^+K^- and $K_s^0K_s^0$

3.2 Partial Wave Analysis of $J/\psi \rightarrow \gamma\pi^+\pi^-$ (preliminary)

Fig. 6 is the invariant mass spectrum of $\pi^+\pi^-$ in $J/\psi \rightarrow \gamma\pi^+\pi^-$. Except for the well

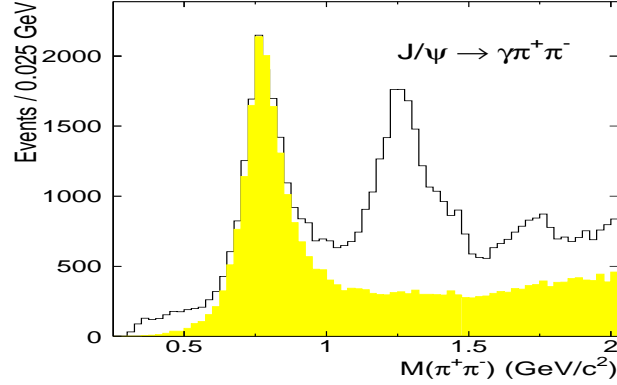


Figure 6: $\pi^+\pi^-$ invariant mass spectrum in $J/\psi \rightarrow \gamma\pi^+\pi^-$

known $f_2(1270)$, a shoulder in the high mass region of $f_2(1270)$ and a bump near 1.7 GeV are seen. PWA is performed to $\pi^+\pi^-$ mass in 1-2 GeV region. 0^{++} and 2^{++} intensity distributions are shown in Fig. 7, where, the same as in $K\bar{K}$ case, dots with error bars are the efficiency corrected data points, solid curves stand for the coherent superposition of the individual Breit-Wigner resonance fit and dashed histograms

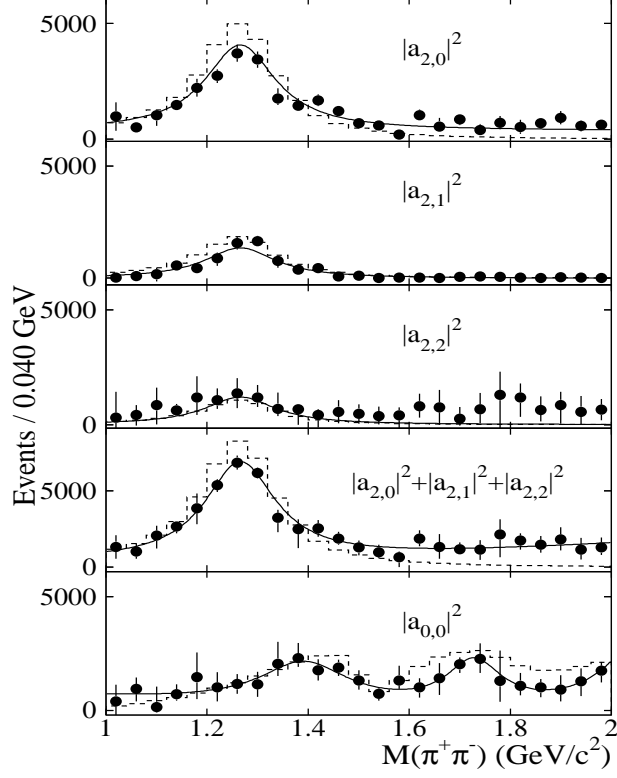


Figure 7: *PWA fit results of $\pi^+\pi^-$*

represent the global fit results. A strong 2^{++} is well determined at around 1.27 GeV, and two 0^{++} 's are observed at around 1.4 and 1.7 GeV. If the 0^{++} at around 1.7 GeV is considered as the same one as in $K\bar{K}$ and the mass and width are fixed to be the values obtained from $K\bar{K}$ analyses, *i.e.*

$$M = 1703_{-10}^{+8} \text{ MeV}, \quad \Gamma = 163_{-22}^{+27} \text{ MeV},$$

the fit results give the masses and widths of 2^{++} and another 0^{++} as:

$$M = 1266 \pm 6 \text{ MeV}, \quad \Gamma = 170_{-30}^{+37} \text{ MeV}$$

$$M = 1383_{-18}^{+20} \text{ MeV}, \quad \Gamma = 274_{-128}^{+59} \text{ MeV}$$

The preliminary results indicate a relative $\pi\pi$ to KK branching ratio of around 30%.

3.3 Measurement of η_c mass

A precise knowledge of the mass difference between $J/\psi(1^{--})$ and $\eta_c(0^{-+})$ charmonium states is useful to the determination of the strength of spin-spin interaction

term in non-relativistic potential model. The mass of J/ψ has been measured with high accuracy, while the η_c mass measurements listed on PDG2000 are very different and the fit to the measurements has a confidence level of only 0.001. Based on BESII $5.8 \times 10^7 J/\psi$ events, we measure the mass of η_c from 6 channels: $J/\psi \rightarrow \gamma\eta_c$, $\eta_c \rightarrow K^+K^-\pi^+\pi^-$, $\pi^+\pi^-\pi^+\pi^-$, $K^\pm K_S^0\pi^\mp$, $\phi\phi$, $K^+K^-\pi^0$ and $p\bar{p}$. Fig. 8 shows η_c signals in above 6 channels. The fit values of the number of events and η_c mass in

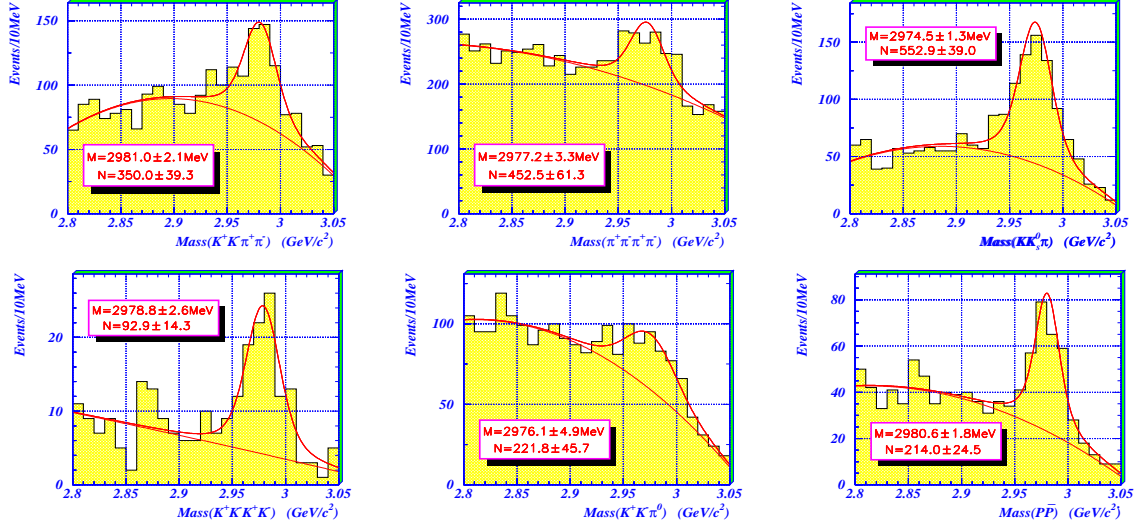


Figure 8: Mass spectra of $K^+K^-\pi^+\pi^-$, $\pi^+\pi^-\pi^+\pi^-$, $K^\pm K_S^0\pi^\mp$, $\phi\phi$, $K^+K^-\pi^0$, $p\bar{p}$

the individual channels are listed in Table 1 (the errors are statistical only). In the fit, the width of η_c is fixed at 16.5 MeV, which is the weighted average of PDG2000, BESI(2000)[7] and recent CLEO two-photon collision experiment [8]. Combine the weighted average with the results from the 5 channels, listed in Table 1, the mass of η_c is given as $M_{\eta_c} = 2977.6 \pm 0.8(\text{stat.}) \text{ MeV}$.

Table 1: Fit values of η_c in the individual channels

Decays	Number of events	M_{η_c} (MeV)
$K^+K^-\pi^+\pi^-$	350.0 ± 39.3	2981.0 ± 2.1
$\pi^+\pi^-\pi^+\pi^-$	452.6 ± 61.3	2977.2 ± 3.3
$K^\pm K_S^0\pi^\mp$	552.9 ± 39.0	2974.5 ± 1.3
$\phi\phi$	92.9 ± 14.3	2978.8 ± 2.6
$p\bar{p}$	214.0 ± 24.5	2980.6 ± 1.8

3.4 Near threshold structure in $J/\psi \rightarrow \gamma p\bar{p}$

There is an accumulation of evidence for anomalous behavior in the $p\bar{p}$ system near $2m_p$ mass threshold. A narrow dip-like structure at a center of mass energy of $2m_p c^2$ was observed in $e^+e^- \rightarrow hadrons$ [9]. A narrow dip structure which is just above $2m_p$ was also observed in diffractive photoproduction of $3\pi^+3\pi^-$ final states[10]. Based on BESII J/ψ data, we analyze $J/\psi \rightarrow \gamma p\bar{p}$. The invariant mass spectrum of $p\bar{p}$ is shown in Fig. 9. Except for η_c signal, there is a clear enhancement near $2m_p$. An S-wave Breit-Wigner function, as shown below, is used to fit the near threshold

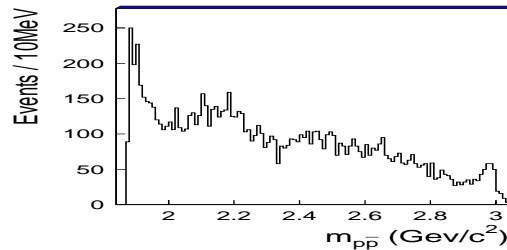


Figure 9: $p\bar{p}$ mass spectrum

enhancement.

$$BW \sim \frac{M_0 \Gamma_0 (q/q_0)}{(M^2 - M_0^2)^2 + (M_0 \Gamma_0 (q/q_0))^2}$$

Where, q is the momentum of daughter particle, q_0 is the momentum of daughter particle at peak. Fig. 10 shows the fit curve. The preliminary fit gives (statistical errors only):

$$M = 1894.1 \pm 1.4 MeV, \quad \Gamma = 48.0 \pm 5.9 MeV$$

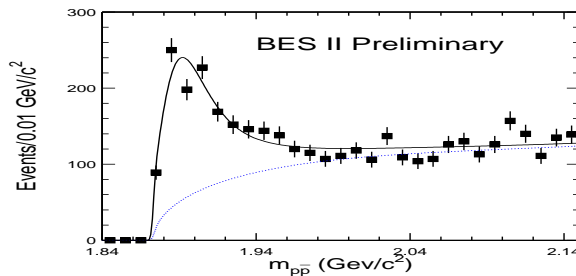


Figure 10: *Fit to $p\bar{p}$ near threshold enhancement*

4 Summary

J/ψ radiative decay is a good laboratory in searches for glueball, the study of light hadron spectroscopy, as well as the glueball spectroscopy. In this talk, we mainly reported the PWA results from $J/\psi \rightarrow \gamma K \bar{K}$, $\gamma \pi^+ \pi^-$, the measurement of η_c and the search for interesting states based on BESII 5.8×10^7 J/ψ data. More analyses are going on and more results will be produced very soon with this data set. CLEO is going to reduce the beam energy to collect a large amount of J/ψ data in a few years. An experimental plan of upgrading BESII/BEPC to BESIII/BEPCII, with a luminosity of 10^{33} and a good detector is underway now. More results on the study of the light hadron spectroscopy and the search of the new form of hadronic states are expected in the near future.

5 Acknowledgements

We acknowledge the staff of the BEPC accelerator and IHEP computing center for their efforts. The work was supported in part by the National Natural Science Foundation of China under Contracts No. 19991480, No. 19825116 and No. 19605007, and by the Department of Energy of US under Contracts No. DE-FG03-93ER40788 (Colorado State University), No. DE-AC03-76SF00515 (SLAC), No. DE-FG03-94ER40833 (University of Hawaii) and No. DE-FG03-95ER40925 (University of Texas at Dallas).

References

1. T. Barnes *et al*, Nucl. Phys., **B224** 241 (1983).
2. N. Isgur *et al*, Phys. Lett., **B124** 247 (1983), Phys. Rev., **D31** 2910 (1985), Phys. Rev. Lett., **54** 869 (1985).
3. L. J. Latorre *et al*, Phys. Lett., **147B** 169 (1984).
4. C. Michael *et al*, Nucl. Phys., **B314** 347 (1989).
G. Bali *et al*, Phys. Lett., **B309** 378 (1993).
C. Morningstar *et al*, Phys. Rev., **D56** 4043 (1997).
5. BES Collaboration, Nucl. Instr. Meth., **A344** 319 (1994).
6. BES Collaboration, Nucl. Instr. Meth., **A458** 627 (2001).
7. BES Collaboration, Phys. Rev., **D62** 072001 (2000).

8. G. Brandenburg *et al*, Phys. Rev. Lett., **85** 3095 (2000).
9. A. Antonelli *et al*, Nucl. Phys., **B517** 3 (1998).
10. P. L. Frabetti *et al* (E687 Collaboration), Phys. Lett., **B514** 240 (2001).